# Combination of Pressure and Temperature Dependent Measurements: A Simple Access to Intrinsic Thermal Activation Energies

**W. Rettig,*,† R. Fritz,‡ and D. Braun†**

*W. Nernst-Institut für Physikalische und Theoretische Chemie, Humboldt-Universität Berlin, Bunsenstrasse 1, D-10117 Berlin, Germany, and BASF Schwarzheide GmbH, Schipkauer Strasse, 1, D-01986 Schwarzheide, Germany*

*Received: January 9, 1997; In Final Form: April 29, 1997*[⊗]

Intrinsic activation energies $E_0^{\#}$ for different adiabatic photoreactions have been derived by combining pressure and temperature dependent time-resolved fluorescence data. This procedure allows the division of the observable activation energy $E_{obs}^{\#}$ into a diffusive barrier $E_d^{\#}$ induced by the solvent viscosity and an intrinsic part $E_0^{\#}$, due to the intramolecular reaction coordinate, and furthermore, the procedure corrects for polarity effects on the rate constant. When applied to the kinetics of charge transfer state formation in DMABN (*N*,*N*-dimethylaminobenzonitrile), it establishes the barrierless nature of the excited state hypersurface in the investigated solute/solvent systems. This case of a negligible intrinsic activation energy is characterized by nonexponential kinetics whereas a comparable case with barrier, the excimer formation in DIPHANT, an intramolecular 9-phenylanthracene excimer molecule, shows exponential decays. For this system in polydimethylsiloxane (S1000), an intrinsic thermal barrier of 17 kJ/mol was determined.

## 1. Introduction

Adiabatic photochemical reactions, such as stilbene isomerization[1−3] or charge transfer state formation in DMABN (N,N-dimethylaminobenzonitrile)[4,5] have been the subject of numerous studies trying to extract activation energies from temperature dependencies of reaction rate constants. In all of these studies, the question arises as to the correct interpretation of these temperature dependencies. There are two main factors which influence the kinetics of adiabatic photoreactions: factor i is diffusion effects induced by the solvent viscosity which slow down large-amplitude reactive motions. They can be described by a hydrodynamic model, either by the well-known Debye−Stokes−Einstein relation or by more refined subsequent theories. They depend mainly on viscosity and its temperature dependence and on the size of the reaction volume[6]. factor ii is kinetic effects caused by an intrinsic thermal barrier. These derive from the relative population of the transition state and therefore depend on temperature and not on viscosity.

For a reaction associated with a large amplitude motion, both sources of temperature variation of the formation rate constant *k* will be active, and the question arises whether the temperature-induced change of the rate constant $k_{temp}$ occurs mainly due to the presence of an intrinsic barrier (factor ii) or more to the viscosity effect (factor i) or to a mixture of both. In such cases, the Arrhenius equation should be written in the form of eq 1

$$\ln k_{temp} = -\frac{E_{obs}^{\#}}{R}\frac{1}{T} + \ln A \qquad (1)$$

where $E_{obs}^{\#}$ stands for the experimentally determined observable derived from a logarithmic plot of the temperature dependent rate constant $k_{temp}$ versus $1/T$. $E_{obs}^{\#}$ is normally interpreted as the activation barrier for the reaction which has to be crossed to proceed from the precursor to the product. With

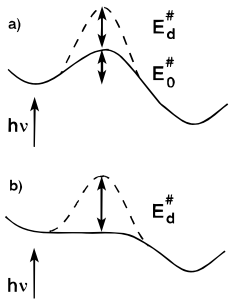


**Figure 1.** Schematic representation of an adiabatic photoreaction involving two states separated by an intrinsic barrier $E_0^{\#}$ and a diffusive one $E_d^{\#}$. a and b denote cases with and without intrinsic barrier.

the additional relation

$$E_{obs}^{\#} = E_0^{\#} + E_d^{\#} = E_0^{\#} + \alpha E_\eta^{\#} \qquad (2)$$

$E_{obs}^{\#}$ can be modeled as the sum of the intrinsic barrier $E_0^{\#}$ and a diffusive or solvent-cage-induced[7] barrier $E_d^{\#}$ (Figure 1). $E_{obs}^{\#}$ contains the intrinsic barrier $E_0^{\#}$, taken in this model as polarity-independent, but even for barrierless reactions the temperature dependence of the viscosity (factor i) leads to a nonzero $E_{obs}^{\#}$ value related to $E_\eta^{\#}$, the activation energy of the solvent mobility. If for a system $E_{obs}^{\#} < E_\eta^{\#}$ is found, this can mostly be interpreted as an indication for $E_0^{\#} \sim 0$.

The schematic representation in Figure 1 shows both possible characteristics of an adiabatic photoreaction consisting of a direct absorbing locally excited state and a product state, which is either a charge transfer or an excimer state for the systems considered here. The transition to the product is determined in (a) by an intrinsic activation energy $E_0^{\#}$, in contrast to (b) which represents the limiting case of an inherent barrierless reaction.

This model separating the overall activation energy into two terms is similar to the quantum-chemical concept of Kasha et al.[7,8] describing the sensitivity of electronic and structral changes of the solute as a function of a perturbation caused by the solvent

* To whom correspondence should be addressed.
† Humboldt-Universität.
‡ BASF Schwarzheide GmbH.
⊗ Abstract published in *Advance ACS Abstracts,* August 1, 1997.

S1089-5639(97)00167-9 CCC: $14.00 

cage. The ability to discriminate between the two cases of Figure 1: possibly arises in systems showing multiple fluorescence: between reaction channels without a viscosity dependent barrier such as the proton-transfer mechanism on the one hand and between a large-amplitude adiabatic photoreaction, on the other hand, which has to cross a solvent-induced barrier, with excimer formation as an example. Only in the latter case can the process be frozen out by increasing the solvent viscosity.

The temperature dependence of the solvent viscosity $\eta$ can be described by the Andrade equation:

$$\ln \eta = \frac{E_\eta^\#}{R}\frac{1}{T} + \ln A_\eta \tag{3}$$

The "barrier" $E_\eta^\#$ of the solvent mobility can be derived using known viscosity data. The underlying molecular process of eq 3 is the viscous flow of a solvent molecule in a solvent environment.

The usual method to separate the intrinsic from the solvent-cage-induced barrier is based on the Kramers equation:

$$k_{\text{isovisc}} = F(\eta)\exp\left(\frac{E_0^\#}{R}\frac{1}{T}\right) \tag{4}$$

where $F(\eta)$ is a viscosity dependent function, which, in the so-called high-viscosity or Smoluchowski limit, is proportional to $\eta^{-1}$. The simplest way is to choose conditions of equal $\eta$, so-called isoviscous conditions: reaction rates in different homologous solvents are compared for temperatures with equal macroscopic viscosity. Then the prefactors $F(\eta)$ should be equal for all the measured points, and the resulting Arrhenius slope should directly reflect $E_0$ provided the following conditions are fulfilled: (i) the microscopic friction is proportional to the macroscopic viscosity. This is, however, not the case in a homologous solvent series due to microviscosity effects which are dependent on the relative size of solute and solvent[6,9] and this ratio can change along the solvent series. (ii) $E_0^\#$ is independent of solvent polarity. This is a good approximation for cases where charge transfer is small or not involved such as valence isomerization or excimer formation. But it could be a pitfall for many well-studied systems such as stilbene isomerization[10−16] and TICT formation in DMABN.[10,17] In this case, methods have to be devised to correct for the polarity dependence of $E_0^\#$.

These corrections are not straightforward and can easily result in misleading conclusions: for DMABN, for example, the TICT reaction was claimed based on a relatively small viscosity range to be completely viscosity independent, and all of the rate changes with temperature were concluded to be due to activated barrier crossing with polarity changes of $E_0^\#$.[10,17] The conclusion of viscosity independence is, however, invalidated by the high-pressure experiments described below where the reaction rate is slowed down through viscosity at constant temperature, although the solvent polarity is increasing and $E_0^\#$ is therefore decreasing.

Following our previous time-resolved measurements of DMABN and other derivatives in highly viscous solvents[18] indicating a negligible intrinsic activation barrier, Drickamer et al. presented static experiments on DMABN in glycerol and other media.[19] They concluded from high-pressure, isothermal fluorescence data that thermal activation accross an intrinsic activation barrier $E_0^\#$ is of a significant contribution. In view of these discrepancies, it is desirable to apply a more reliable method of separating $E_\text{d}^\#$ and $E_0^\#$, giving a simple means of determining whether $E_0^\#$ equals to zero in a given system. An early approach[20] is the isothermal viscosity variation at constant temperature in solvent mixtures of a weakly and a strongly viscous solvent (e.g., glycerol/water solvent) with, in the ideal case, equal polarity. However, microscopic friction may still depend differently on composition than on the macroscopic viscosity due to the different sizes of solvent molecules. It is therefore preferable to increase the viscosity at constant temperature by increasing the hydrodynamic pressure in a single solvent: in this case, microviscosity effects can be largely avoided.

To reach a satisfactory description of the experimental results, these should also be discussed in terms of the activation volumes $\Delta V^\#$ connected with the reaction, analogously to the activation energy. In studying the pressure dependence of the solvent viscosity $\eta$ Hirai and Eyring described the solvent as a discontinuous medium, where "solvent hole" volume reflecting in $\Delta V^\#$ is necessary for a diffusion process.[21,22] Data derived

$$\left.\frac{\partial \ln\dfrac{\eta(P_0)}{\eta(P)}}{\partial P}\right|_{T=\text{const}} = -\frac{1}{RT}\Delta V^\# \tag{5}$$

via equations similar to eq 5, where $\eta$ is replaced by rate constants or reaction quantum yields will clarify, whether the intramolecular motion of a solute engaged in an adiabatic photoreaction and the diffusion in the pure solvent are of a similar nature or not.

## 2. Method

Here we wish to indroduce an improved approach, the comparison of reaction rates for isoviscous conditions in a single solvent where the reaction rates are slowed down (i) by increasing viscosity at constant temperature by using rate constants $k_\text{press}$ from high-pressure experiments and (ii) by decreasing temperature (low-temperature effect, rate constant $k_\text{temp}$), which also increases solvent viscosity. It is necessary to find a common scale for both data sets of pressure- ($k_\text{press}$) and temperature-dependent rate constants ($k_\text{temp}$), which is naturally the viscosity scale.

By combining eqs 1−3, the Arrhenius and Andrade equations, $k_\text{temp}$ can be expressed as a function of the solvent viscosity $\eta$:

$$\ln k_{temp} = -\frac{E_0^\# + E_d^\#}{E_\eta^\#}\ln \eta + \ln A + \frac{E_0^\# + E_d^\#}{E_\eta^\#}\ln A_\eta = -\frac{E_{obs}^\#}{E_\eta^\#}\ln \eta + \text{const} \tag{6}$$

Of interest is the first term of the right hand side showing the dependence on the viscosity; the rest can be summarized into a constant. An analogous equation for the rates $k_\text{press}$ is easily derived, if we take into account that all thermally activated

$$\ln k_\text{press} = -\frac{E_d^\#}{E_\eta^\#}\ln \eta + \text{const}' \tag{7}$$

processes can be excluded because $k_\text{press}$ is measured at constant temperature.

If $k_\text{press}$ and $k_\text{temp}$ are equal for a range of different viscosities (Figure 2b), then the intrinsic barrier $E_0^\#$ can be concluded to be equal to zero within experimental uncertainty. This is equivalent to the absence of an intrinsic temperature effect. The observed temperature dependence of the rate constant is then a pure viscosity effect beside the influence of polarity changes. A thermal activation can be excluded. If there is a difference between $k_\text{press}$ and $k_\text{temp}$ indicating an intrinsic barrier, the slope

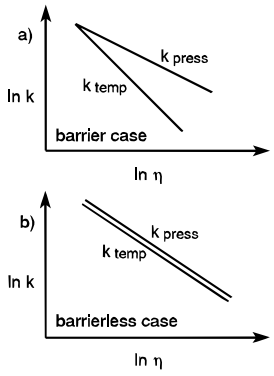


**Figure 2.** Schematic comparison of the rate constants $k_{press}$ and $k_{temp}$ of an ideal system (a) with and (b) without an intrinsic barrier $E_d^{\#}$.

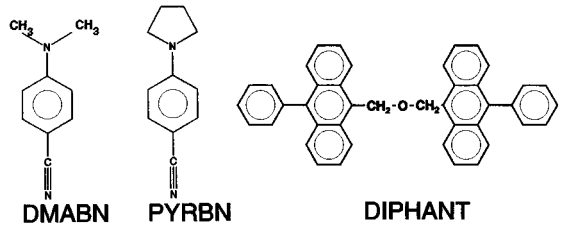


**Figure 3.** Formulas and abbreviations of the investigated compounds.

of the rate constant ratio allows directly to extract the $E_0^{\#}$ value (Figure 2a). This ratioing approach also allows to correct for the polarity influence of the rate constant, based on the assumption that constant viscosity implies constant polarity for a given solvent.

Here, we wish to test this approach by comparing the system DMABN with vanishing $E_0^{\#}$ [18] to another system with a nonzero intrinsic barrier, in this case an intramolecular excimer.

## 3. Experimental Section

Dimethylaminobenzonitrile (DMABN) and pyrrolidinobenzonitrile (PYRBN) were the same compounds used previously,[23] and the intramolecular excimer DIPHANT, two phenylanthracenes linked by an oxymethylene chain with three units (Figure 3), was a gift from H. Bouas-Laurent. This compound has often been used as a viscosity probe in highly viscous liquids or polymers.[24−26]

The solvents glycerol triacetate (GTA) and glycerol were obtained commercially from MERCK and were nonfluorescent after purification at the sensitivity levels used. GTA was purified by distillation under reduced pressure over anhydrous $Na_2CO_3$. For DIPHANT, a synthetic oil was used, polydimethylsiloxane of a macroscopic viscosity $\eta = 1000$ mPa s (S1000) at 298 K which was received from Rhône Poulenc. This latter solvent contained some fluorescent impurity with a long lifetime which could easily be separated from the short-lived fluorescence of DIPHANT in the time-resolved experiments.

Fluorescence decay traces were measured with a single photon-counting equipment described elsewhere[27] using synchrotron radiation from BESSY (single-bunch mode) as excitation source. The high-pressure equipment has been described previously.[18,28] The fluorescence decays $F(t)$ were fitted using the least-squares iterative reconvolution technique and a multiexponential model function:

$$F(t) = \sum_i \alpha_i \exp\left(-\frac{t}{\tau_i}\right) \tag{8}$$

All the curves could be fitted satisfactorily ($\chi^2$ around 1.2 or below) by utilizing $n = 3$ exponents or less. From the

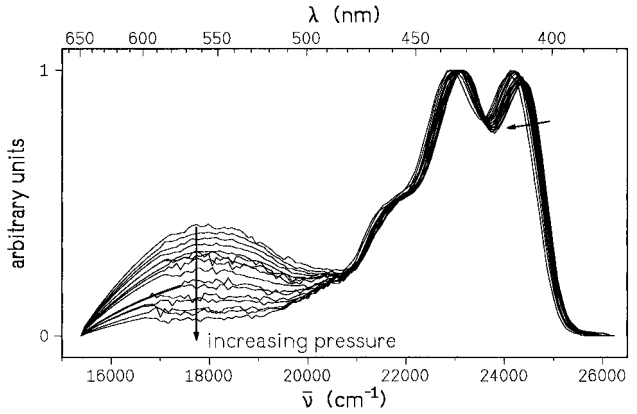


**Figure 4.** Pressure dependent stationary fluorescence spectra from 1 to 3750 bar of the system DIPHANT in S1000 at room temperature. Spectra are normalized with respect to their band maximum. The arrows indicate increasing pressure.

multiexponential expansion of the nonexponential decays, mean decay times $\langle\tau\rangle$ corresponding to the precursor survival probabilities $\int Q(t)\, dt$ [29] were calculated according to eq 9.

$$\langle\tau\rangle = \frac{\sum_i \alpha_i \tau_i}{\sum_i \alpha_i} \tag{9}$$

The average reaction rate constants were calculated by $k = \langle\tau\rangle^{-1} - \tau_{77K}^{-1}$ where the reference temperature 77 K was chosen such that the decay times had reached their limiting upper value with corresponding monoexponential decay behavior.

The excimer system DIPHANT in S1000 can be satisfactorily analyzed by a monoexponential term in the temperature and pressure range investigated here. By global analysis, it was documented that this system is in the irreversible limit under these conditions; no back reaction from the excimer occurs.[28]

## 4. Results

In Figure 4, the static fluorescence spectra of the excimer system DIPHANT in the oil S1000 as a function of pressure at constant temperature are presented as an example. The same qualitative effects (i.e., decrease of the relative product band intensity at long wavelength) could be observed in the investigated dual fluorescent TICT-forming compounds. The measurement under isothermal conditions allows us to neglect all internal thermal activation processes, and only the dependence on the diffusion barrier $E_d^{\#}$ linked to the solvent viscosity remains. The structured fluorescence band of the primary absorbing locally excited state is situated in the high-energy region. The red shift of the band maximum with increasing pressure indicates the growing polarizability of the solvent environment.

Our goal in measuring fluorescence decays for the various systems is to produce two different kinetic data sets, one as a function of temperature $k_{temp}$ and the other one as a function of pressure $k_{press}$ at constant temperature. Let us first present these sets separately in order to demonstrate the kind of information which can be obtained, before the advantages of combining both sets are considered.

Using eq 5 for the pressure dependent rate constants $k_{press}$, the activation volumes $\Delta V^{\#}$ are calculated and shown in Table 1. The $\Delta V^{\#}$ values for the pure solvents are determined based on the pressure dependent viscosity data in the literature.[30,31] It can be concluded from Table 1 that the diffusion process of the pure solvent necessitates considerably more reactive volume

**TABLE 1: Activation Volumes $\Delta V^{\#}$ at 300 K from High-Pressure Experiments Including the Correlation Coefficient $r^2$ of the Linear Regression[a]**

| system | pure glycerol | DMABN/glycerol | pure GTA | DMABN/GTA | PYRBN/GTA | pure S1000 | DIPHANT/S1000 |
|---|---|---|---|---|---|---|---|
| $\Delta V^{\#}$/cm$^3$ mol$^{-1}$ | 12.9 | 7.3 | 57.2 | 13.6 | 13.9 | 25.0 | 25.0 |
| $\Delta V^{\#}$/Å$^3$ | 21.0 | 12.1 | 95.0 | 22.6 | 23.0 | 41.0 | 41.0 |
| $r^2$ | 0.99 | 0.97 | 0.99 | 0.98 | 0.99 | 0.97 | 0.98 |

[a] In the solvent GTA, the upper limit of the pressure range is 2.5 kbar, in glycerol 5 kbar, in S1000 3.5 kbar.

**TABLE 2: Results of the Arrhenius Plots of the Investigated Systems[a]**

| system | $E^{\#}_{obs}$/kJ mol$^{-1}$ | log ($A$/s$^{-1}$) | $r^2$ |
|---|---|---|---|
| DIPHANT/S1000 | 24 ± 2 | 12.5 ± 0.9 | 0.97 |
| DMABN/glycerol | 35 ± 2 | 15.9 ± 0.8 | 0.98 |
| DMABN/GTA | 29 ± 2 | 14.8 ± 0.8 | 0.97 |
| PYRBN/glycerol | 32 ± 2 | 15.4 ± 0.8 | 0.96 |
| PYRBN/GTA | 29 ± 2 | 14.7 ± 0.8 | 0.98 |

[a] In glycerol, a temperature range from −40 to +40 °C, in GTA from −40 to +20 °C, and in S1000 from −65 to +45 °C, is considered.

**TABLE 3: Slopes Corresponding to Equations 6 and 7 Including the Activation Energies $E^{\#}_{\eta}$ for the Solvent Mobility**

| system | $(E^{\#}_0 + E^{\#}_d)/E^{\#}_{\eta}$) temp | $(E^{\#}_d/E^{\#}_{\eta})$ press | $E^{\#a}_{\eta}$/kJ mol$^{-1}$ |
|---|---|---|---|
| DMABN/glycerol | 0.60 | 0.55 | 54.0 |
| DMABN/GTA | 0.21[b] | 0.21[b] | > 50.0 |
| | 0.35[c] | 0.30[c] | |
| DIPHANT/S1000 | 1.42 | 0.72 | 17.0[d] |

[a] Reference 31. [b] Low-viscosity range. [c] High-viscosity range, Figure 6. [d] Based on viscosity data of Rhône Poulenc.

as compared to the rotational motion in the TICT-forming molecules in contrast to the excimer compound. Taking into account the large size of the solvent molecules, it is obvious that a place exchange motion in the pure solvent needs more volume than the intramolecular rotational diffusion of subgroups of the solute necessary for TICT formation. In glycerol, $\Delta V^{\#}$ of the pure solvent viscosity is two times larger than that measured for DMABN. In GTA, this factor increases to around 4, which indicates a correlation to the increased size of the solvent molecule. For DMABN and PYRBN, similar results are found which suggests a negligible influence of the dialkylamino rotor size on the activation volume.

Table 2 summarizes the activation energies $E^{\#}_{obs}$ which still contain both polarity and viscosity influences, in addition to the intrinsic barrier derived from Arrhenius plots of the rate constants $k_{temp}$. Similar to those values from pressure experiments, the $E^{\#}_{obs}$ values for DMABN and PYRBN are equal within experimental error. Comparing the $E^{\#}_{obs}$ values with the activation energies $E^{\#}_{\eta}$ of the solvent mobilities in Table 3, it is obvious that the excimer system DIPHANT in S1000 shows a significantly larger experimental activation barrier $E^{\#}_{obs} = E^{\#}_0 + E^{\#}_d$ than the corresponding $E^{\#}_{\eta}$ value. The TICT-forming compounds, on the other hand, exhibit significantly smaller $E^{\#}_{obs}$ values compared with $E^{\#}_{\eta}$ of GTA and glycerol, similar to those previously for low-viscosity solvents.[5] These results are a first indication of an intrinsic barrierless reaction in these TICT systems, while the excimer compound shows a significant intrinsic activation barrier, which will be quantified in the next step of the evaluation. For GTA, only a lower limit is presented in Table 3 because its viscosity cannot be linearly described according to eq 3 in the temperature range investigated. Thus, the activation energy $E^{\#}_{\eta}$ of GTA can be regarded as a temperature dependent value. This deviation from eq 3 can be traced back to the fact that the lower temperature limit of the measurements is near to the glass transition point of GTA.

In the next step, we combine the data sets and plot $k_{temp}$ and $k_{press}$ on a common viscosity scale in a double logarithmic representation (Figures 5 and 6). From the slopes, the ratios $(E^{\#}_0 + E^{\#}_d)/E^{\#}_{\eta}$ and $E^{\#}_d/E^{\#}_{\eta}$, according to eqs 6 and 7, are determined and summarized in Table 3. As shown in Figure 6, the data of DMABN in GTA have to be evaluated in two different nearly linear viscosity ranges. But although there are small differences in the slopes of $k_{press}$ and $k_{temp}$ for the systems DMABN in glycerol and DMABN in GTA (high-viscosity range), the resulting $E^{\#}_0$ values are very small, comparable to the thermal energy $kT$, consistent with a negligible intrinsic barrier.

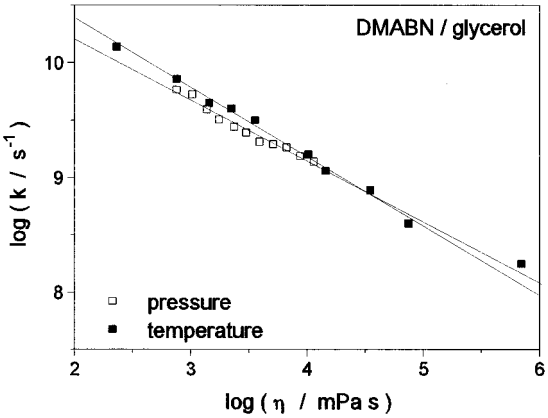


**Figure 5.** Rate constants $k_{temp}$ and $k_{press}$ of DMABN in glycerol measured as a function of pressure at 300 K and as a function of temperature presented on a common viscosity scale.

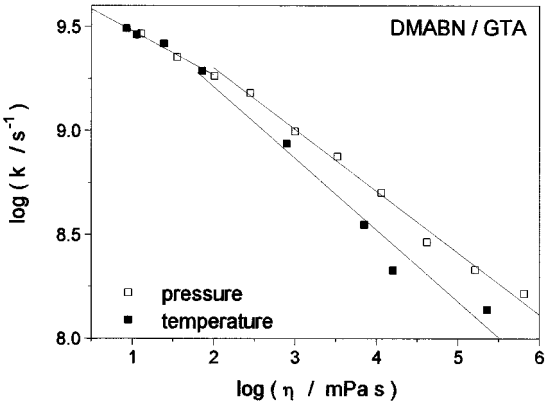


**Figure 6.** Rate constants $k_{temp}$ and $k_{press}$ of DMABN in GTA measured as a function of pressure at 300 K and as a function of temperature presented on a common viscosity scale.

The comparison of temperature and pressure dependencies can most easily be done by plotting the ratio $k_{temp}/k_{press}$ as a function of solvent viscosity on a double-logarithmic scale, see Figure 7. This has the advantage that, as the logarithm of the viscosity is usually proportional to $T^{-1}$, eq 3, this plot closely resembles a scaled Arrhenius plot, with the difference that effects other than those of temperature changes are eliminated because isopolar/isoviscous conditions are compared. This kind of combining eqs 6 and 7 leads directly to the ratio $E^{\#}_0/E^{\#}_{\eta}$:

$$\ln \frac{k_{temp}}{k_{press}} = -\frac{E^{\#}_0}{E^{\#}_{\eta}} \ln \eta + \text{const}'' \qquad (10)$$

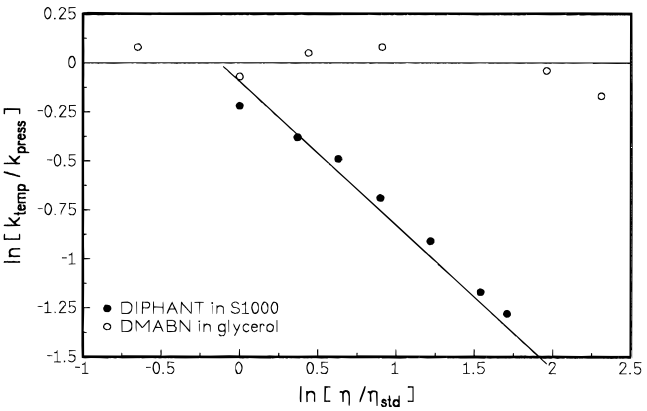


**Figure 7.** Representation of the logarithm of the ratio $k_{temp}/k_{press}$ for the systems DMABN in glycerol and DIPHANT in S1000 on a rescaled logarithmic viscosity axes. $\eta_{std}$ are the viscosities at standard conditions (298 K, 1 bar). The values of $k_{press}$ are interpolated.

With the knowledge of $E_\eta^\#$, it is possible to extract the intrinsic activation energies $E_0^\#$ from the observed slopes. The horizontal slope determined for DMABN is an indication for a barrierless intrinsic reaction profile. The intrinsic barrier $E_0^\#$ for the excimer system DIPHANT in S1000 on the other hand is found to be 11.9 kJ mol$^{-1}$, similar to the diffusional barrier $E_d^\#$, 12.2 kJ mol$^{-1}$ (Table 3). The sum of both values is in good accordance with the result of the Arrhenius plot $E_{obs}^\#$ in Table 2. Thus, the assumption formulated in eq 2 leads to satisfying results. Especially for the excimer system, the overall activation energy $E_{obs}^\#$ could be separated into two components, the intrinsic thermal and the viscosity-induced diffusional part.

## 5. Discussion

**5.1. Nonexponential Decays on Barrierless Potentials.** The nonexponential decays observed for DMABN and PYRBN are a direct consequence of the barrierless potential involved. The "staircase" model of Bagchi et al.[32,33] can be satisfactorily used to describe the nonexponential nature of the decays. The staircase potential consists of a flat part of width *a* with reflective boundary condition at one side ("step up") and total absorbing boundary condition at the other side ("step down"), modeling the reaction. It is very close to the Ooster−Nishyima model defined by absorbing boundary conditions at both sides.[34] The staircase model has been successfully applied to DMABN and derivatives[35,36] and can explain the strong polarity dependence of the rate constants by a polarity variation of the flat potential range *a*. In solvents of larger polarity, the width *a* becomes smaller. This is the consequence of a conical intersection on the reaction pathway between the less polar precursor and the highly polar TICT state which is more efficiently stabilized by the polar solvent.[35,37−40]

**5.2. Fractional Viscosity Dependence and the Reaction Volume.** In contrast to DMABN and PYRBN, DIPHANT possesses a nonzero intrinsic activation energy $E_0^\#$ which is probably related to the conformational changes necessary within the linking oxymethylene chain. As a result of the intrinsic barrier, the observed decays are monoexponential, supporting the above view of the connection of nonexponentiality with a barrierless potential. Nevertheless, both types of reactions, TICT and excimer formation, are large-amplitude motions and are thus subject to strong viscosity dependencies. The reaction volume required for DIPHANT can even be judged considerably larger than for DMABN.[41,42] In this case, the Debye−Stokes−Einstein relation with a linear viscosity dependence ($\alpha = 1$) is expected to hold better than for DMABN. This means that the diffusive barrier $E_d^\#$ approaches $E_\eta^\#$ or that the coefficient $\alpha$ in eq 2 converges to 1. In fact, excimer systems are known to follow better the linear viscosity dependencies[43,44] in contrast to systems showing a torsional relaxation process in the excited state.[45,46] For the excimer system studied here (translational diffusion of phenylanthracene moieties), the ratio $E_d^\#/E_\eta^\#$ is significantly larger than that for systems with smaller reaction volumes like DMABN (intramolecular rotational diffusion of dialkylamino and benzonitrile groups against each other) which do not see the full macroscopic friction. Their microscopic friction is more strongly reduced, and $\alpha = E_d^\#/E_\eta^\#$ can be much smaller than 1 (Table 3). For a negligible intrinsic barrier, this leads to $E_{obs}^\#$ values which are significantly smaller than $E_\eta^\#$, as previously reported.[5,47] The complications due to the additional polarity changes will be discussed below. Equation 2 is usually cast in the form of eq 11[6] which clearly shows the connection to eq 7.

$$k \propto \eta^{-\alpha} \tag{11}$$

It can be seen that a fractional viscosity dependence ($\alpha < 1$) can be an indication of microviscosity effects, especially the solute/solvent ratio, and $\alpha$ can be correlated with the reaction volume necessary for the reactive internal motion within the solute and the diffusion process of the pure solvent. For some adiabatic photoreactions which require a very small reaction volume and are not connected with electron transfer, such as excited state proton transfer (ESIPT), the viscosity dependence is in fact very weak, and $\alpha$ is correspondingly much smaller than 1.[48]

In deriving $\alpha$ values, care should be taken to avoid combining the results measured in different solvents, as is normally done in isoviscosity plots using homologous solvent series. This pitfall has recently been shown for *cis*-stilbene isomerization: pressure experiments in a single solvent lead to $\alpha = 1$, whereas isothermal viscosity changes by using different solvents result in $\alpha < 1$.[49]

**5.3. Polarity Effects and Isolation of Temperature-Induced Rate Changes.** The approach of ratioing the temperature and the pressure induced variations of the rate constant corrects for several factors: of the four variables which are most important for charge transfer reactions with or without barrier—temperature, solvent viscosity, solvent dielectric relaxation behavior, and solvent polarity—the latter three behave in an almost parallel way upon cooling or upon increasing pressure. This points to the importance of density effects as controlling "supervariable".

If the assumption is made that solvent density changes induced by pressure or temperature lead to similar changes of solvent viscosity, relaxation time, and polarity, then the ratioing of rate constants for equal viscosity will not only correct for the viscosity but also for the polarity effects. This is especially important for TICT formation in DMABN and related compounds where the rate constants depend strongly on polarity.[10,17,35,40,50,51] Due to this effect, the activation volumes and Arrhenius slopes discussed above for the TICT compounds have to be viewed with caution (see below), but the combined temperature and pressure data are expected to yield the correct results.

The pressure-induced decrease of the rate constants (Figures 5 and 6) is not a full viscosity effect but is counteracted by the polarity increase which increases the rates. The observed pressure dependencies are thus expected to be weaker than predicted on the basis of the Kramers−Smoluchowski limit ($\alpha = 1$). This is exemplified by the present data (Table 3) and by corresponding data on various other CT systems with pressure variation.[45,46] This can also yield an explanation for the small

activation energies in the low-temperature experiments, Table 3 and refs 5 and 52, where $E_{obs} < E_\eta$. The refs 13 and 49 contain pressure data for different temperatures, which allow even a more refined treatment. From the set of data, viscosity-free polarity dependent intrinsic activation energies can be determined as a function of density/viscosity by combining isoviscous conditions for different temperatures. This procedure necessitates, for meaningful Arrhenius slopes, high-pressure data sets for several temperatures. The approach presented here is a simplification and needs only two data sets, one temperature and one pressure run. It leads to the viscosity/polarity-free intrinsic activation energy but cannot yield activation energies as a function of solvent viscosity as the method in refs 13 and 49.

It has been claimed that the viscosity influence on the rate constant of TICT formation in DMABN is negligible[10,17] and that main effects are barrier height changes induced by changes of polarity. On the other hand, we have shown here that, at least for the solvents GTA and glycerol,[18] the barrier is nonexistent, and the temperature and pressure-induced changes are viscosity effects counteracted by polarity effects. These conflicting views can be reconciled by a reinterpretation of the data of Hicks et al.[10,17] In their approach, they claimed all the observed variations to be due to barrier-height changes. We have shown that the opposite view, i.e., polarity-induced changes of the preexponential factors on a barrierless potential,[35] can equally well explain the observed data and is consistent with nonexponential decays[36] and the pressure data reported here and in ref 18.

## 6. Conclusions

A methodical approach combining high-pressure and low-temperature experiments has been introduced which allows the following conclusions to be drawn. The observable activation energy $E^{\#}_{obs}$ can be separated into a diffusive barrier $E^{\#}_{d}$ and a thermally activated, intrinsic part $E^{\#}_{0}$. The TICT-forming compounds DMABN and PYRBN in the highly viscous solvents GTA (medium polar) and glycerol (highly polar) are of barrierless nature in contrast to the excimer system DIPHANT in the synthetic oil S1000, for which an inherent barrier of 17 kJ/mol is derived. The diffusional activation energy $E^{\#}_{d}$ for all investigated systems shows smaller values than the activation energy $E^{\#}_{\eta}$ of the solvent mobility. This can be traced back to the different nature of the molecular processes described by $E^{\#}_{d}$ (solute reactive diffusion) and $E^{\#}_{\eta}$ (diffusion of a solvent molecule).

**Acknowledgment.** We thank the DFG for financial support (Grant Sfb 337), H. Bouas-Laurent (Bordeaux) for providing the compound DIPHANT, and K. Hara (Kyoto) and J. Schroeder (Göttingen) for valuable advice regarding the high-pressure equipment.

## References and Notes

(1) Waldeck, D. H. *Chem. Rev.* **1991**, *91*, 415.
(2) Saltiel, J.; D'Agostino, J.; Megarity, E. D.; Metts, L.; Neuberger, K. R.; Wrighton, M.; Zafiriou, O. C. In *Organic Photochemistry*; Chapman, O. L., Ed.; Marcel Dekker, Inc.: New York, 1971; Vol. 3, p 1.
(3) Saltiel, J.; Sun, Y.-P. *J. Phys. Chem.* **1989**, *93*, 6246. Saltiel, J.; Sun, Y.-P. *Photochromism—Molecules and Systems*; Dürr, H.; Bouas-Laurent, H., Eds.; Elsevier: Amsterdam, 1990; p 64.
(4) Grabowski, Z. R.; Rotkiewicz, K.; Siemiarczuk, A.; Cowley, D. J.; Baumann, W. *Nouv. J. Chim.* **1979**, *3*, 443.
(5) Lippert, E.; Rettig, W.; Bonačič-Koutecký, V.; Heisel, F.; Miehé, J. A. *Adv. Chem. Phys.* **1987**, *68*, 1.
(6) Alwattar, A. H.; Lumb, M. D.; Birks, J. B. In *Organic Molecular Photophysics*; Birks, J. B., Ed.; Wiley: New York, 1973; Vol. 1, Chapter 8.
(7) Dellinger, B.; Sytnik, A.; Kasha, M. *Pure Appl. Chem.* **1993**, *65*, 1641.
(8) Heldt, J.; Gormin, D.; Kasha, M. *Chem. Phys.* **1989**, *136*, 321.
(9) Gierer, A.; Wirtz, K. *Z. Naturforsch.* **1953**, A*8*, 532.
(10) Hicks, J. M.; Vandersall, M. T.; Sitzmann, E. V.; Eisenthal, K. B. *Chem. Phys. Lett.* **1987,** *135*, 413.
(11) Sundström, V.; Gillbro, T. *Chem. Phys. Lett.* **1984**, *109*, 538.
(12) Sundström, V.; Gillbro, T. *Ber. Bunsen-Ges. Phys. Chem.* **1985**, *89*, 222.
(13) Schroeder, J.; Schwarzer, D.; Troe, J.; Vöhringer, P. *Chem. Phys. Lett.* **1994**, *218*, 43.
(14) Troe, J. *Ber. Bunsen-Ges. Phys. Chem.* **1991**, *95*, 228.
(15) Schroeder, D. *Ber. Bunsenges. Phys. Chem.* **1991**, *95*, 233.
(16) Schroeder, J.; Troe, J.; Vöhringer, P. *Chem. Phys. Lett.* **1993**, *203*, 255.
(17) Hicks, J. M.; Vandersall, M. T.; Babarogic, Z.; Eisenthal, K. B. *Chem. Phys. Lett.* **1985**, *116*, 18.
(18) Braun, D.; Rettig, W. *Chem. Phys.* **1994**, *180*, 231.
(19) Lang, J. M.; Dreger, Z. A.; Drickamer, H. G. *Chem. Phys. Lett.* **1995**, *243*, 78. Dreger, Z. A.; Lang, J. M.; Drickamer, H. G. *J. Phys. Chem.* **1996**, *100*, 4646.
(20) Förster, T.; Hoffmann, G. *Z. Phys. Chem. (Munich)* **1971**, *75*, 63.
(21) Glasstone, S.; Laidler, K. J.; Eyring, H. In *The Theory of Rate Processes*; McGraw-Hill: New York, 1941.
(22) Dreger, Z. A.; Lang, J. M.; Drickhamer, H. G. *Chem. Phys.* **1992**, *166*, 193.
(23) Rettig, W. *J. Lumin.* **1981**, *26*, 21.
(24) Bokobza, L.; Pajot-Augy, E.; Monnerie, L.; Castellan, A.; Bouas-Laurent, H.; Millet, C. *Polymer* **1983**, *24*, 117.
(25) Bokobza, L.; Pajot-Augy, E.; Monnerie, L.; Castellan, A.; Bouas-Laurent, H. *Polym. Photochem.* **1984**, *5*, 191.
(26) Bokobza, L.; Pajot-Augy, E.; Monnerie, L.; Castellan, A.; Bouas-Laurent, H. *Macromolecules* **1984**, *17*, 1490.
(27) Vogel, M.; Rettig, W. *Ber. Bunsen-Ges. Phys. Chem.* **1987**, *91*, 1241.
(28) Fritz, R. *Ph.D. Thesis*, Technical University of Berlin; Köster Verlag: Berlin, 1994, ISBN 3−929937-57-3.
(29) Nadler, W.; Marcus, R. *J. Chem. Phys.* **1987**, *86*, 3906.
(30) Groubert, E.; Charles, E. *C. R. Acad. Sci.* **1969**, *269*, 1454.
(31) Landolt-Börnstein, (*Zahlenwerte und Funktionen aus Physik, Chemie, Astronomie, Geophysik und Technik*; Springer: Berlin, 1969; Vol 2.
(32) Bagchi, B.; Fleming, G. R. *J. Phys. Chem.* **1990**, *94*, 9.
(33) Bagchi, B. *Chem. Phys. Lett.* **1987**, *135*, 558.
(34) Oster, G.; Nishijima, N. J. *J. Am. Chem. Soc.* **1956**, *78*, 1581.
(35) Rettig, W. *Ber. Bunsen-Ges. Phys. Chem.* **1991**, *95*, 259.
(36) Braun, D.; Rettig, W. *Chem. Phys. Lett.* **1997**, *268*, 110.
(37) Rettig, W.; Wermuth, G. *J. Photochem.* **1985**, *28*, 351.
(38) Rettig, R. *Angew. Chem., Int. Ed. Engl.* **1986**, *25*, 971.
(39) Rettig, W. In *Topics in Current Chemistry*, *Electron Transfer I*; Mattay, J., Ed.; Springer Verlag: Berlin, 1994; Vol. 169, p 253.
(40) Rettig, W. In *Dynamics and Mechanisms of Photoinduced Electron Transfer and Related Phenomena*; Mataga, N., Okada T., Masuhara, H., Eds.; Elsevier Science Publishers B. V.: Amsterdam, 1992; p 57.
(41) Rettig, W.; Baumann, W. In *Photochemistry and Photophysics*; Rabek, J. F., Ed.; CRC Press, Inc: Boca Raton, 1992; Vol. 6, p 79.
(42) Rettig, W.; Lapouyade, R. In *Topics in Fluorescence Spectroscopy IV: Probe Design and Chemical Sensing*; Lakowicz, J. R., Ed.; Plenum Press: New York, 1994; p 109.
(43) Hara, K.; Yano, H. *J. Phys. Chem.* **1988**, *90*, 4265.
(44) Hara, K.; Yano, H. *J. Am. Chem. Soc.* **1988**, *110*, 1911.
(45) Bulgarevich, D. S.; Kajimoto O.; Hara, K. *J. Phys. Chem.* **1995**, *99*, 13356.
(46) Hara, K.; Kometani, N.; Kajimoto O. *J. Phys. Chem.* **1996**, *100*, 1488.
(47) Heisel, F.; Miehé, J. A.; Martinho, J. M. G. *Chem. Phys.* **1985**, *98*, 243.
(48) Salman, O. A.; Drickamer, H. G. *J. Chem. Phys.* **1981**, *75*, 572.
(49) Nikowa, L.; Schroeder, J.; Schwarzer, D.; Troe, J. *J. Chem. Phys.* **1992**, *97*, 4827.
(50) Su, S.-G.; Simon, J. D. *J. Chem. Phys.* **1988**, *89*, 908.
(51) Simon, J. D.; Doolen, R. *J. Am. Chem. Soc.* **1992**, *114*, 4861.
(52) Heisel, F.; Miehé, J. A. *Chem. Phys.* **1985**, *98*, 233.